

**Binding of permanganate anion to pentaammineazidocobalt(III) cation in solution and solid phases: synthesis, characterization, X-ray structure and geneotoxic effects of  $[\text{Co}(\text{NH}_3)_5\text{N}_3](\text{MnO}_4)_2 \cdot \text{H}_2\text{O}$**

Ritu BALA<sup>1,\*</sup>, Jinkwon KIM<sup>2</sup>, Vinit PRAKASH<sup>3</sup>

<sup>1</sup>Department of Chemistry, Guru Nanak Dev University, Amritsar, Punjab, India

<sup>2</sup>Department of Chemistry, Kongju National University, Shinkwan, Kongju, Chungman, South Korea

<sup>3</sup>Department of Chemistry, Maharishi Markandeshwar University, Sadopur, Ambala, Haryana, India

\*Correspondence: [rituhatta@yahoo.com](mailto:rituhatta@yahoo.com)

ORCIDs:

RITU BALA: <https://orcid.org/0000-0002-8520-0399>

JINKWON KIM: <https://orcid.org/0000-0003-0109-7126>

VINIR PRAKASH: <https://orcid.org/0000-0002-7829-151X>

Cite as: Bala R, Kim J, Prakash V. Binding of permanganate anion to pentaammineazidocobalt(III) cation in solution and solid phases: synthesis, characterization, X-ray structure and geneotoxic effects of  $[\text{Co}(\text{NH}_3)_5\text{N}_3](\text{MnO}_4)_2 \cdot \text{H}_2\text{O}$ . Turkish Journal of Chemistry. doi: 10.3906/kim-2012-66

**Abstract:** A pentaammineazidocobalt(III) complex,  $[\text{Co}(\text{NH}_3)_5\text{N}_3](\text{MnO}_4)_2 \cdot \text{H}_2\text{O}$  has been synthesized by an one-pot synthesis method. It was characterized by spectroscopic studies like IR and UV-visible. The single crystal X-ray structure analysis revealed that title complex crystallizes in space group Cc. The cobalt center is six coordinated with slightly octahedral geometry. The supramolecular architecture is also formed by intermolecular N-H...O (anion and  $\text{H}_2\text{O}$ ) and Mn-O...O-H hydrogen bonds. The binding property of cation,  $[\text{Co}(\text{NH}_3)_5\text{N}_3]^{2+}$  with anion,  $\text{MnO}_4^-$  has also been determined (in solution phase) with the help of UV-visible spectroscopic titrations. Further, the genotoxic effects of  $\text{KMnO}_4$ ,  $[\text{Co}(\text{NH}_3)_5\text{N}_3]\text{Cl}_2$  and  $[\text{Co}(\text{NH}_3)_5\text{N}_3](\text{MnO}_4)_2 \cdot \text{H}_2\text{O}$  were studied using *Allium cepa* root chromosomal aberration assay and it revealed that the genotoxicity of the newly synthesized complex is 1.97 - 1.76 fold, which is less as compared to  $\text{KMnO}_4$ . The order of genotoxic potential has been observed to be  $\text{KMnO}_4 > [\text{Co}(\text{NH}_3)_5\text{N}_3](\text{MnO}_4)_2 \cdot \text{H}_2\text{O} > [\text{Co}(\text{NH}_3)_5\text{N}_3]\text{Cl}_2$ .

**Key words:** Anion binder, pentaammineazidocobalt(III), coordination chemistry, genotoxicity, IR spectroscopy, X-ray crystallography

## 1. Introduction

Potassium permanganate is an exceptionally strong oxidizing agent violet coloured, crystalline, odorless substance and easily available from any pharmaceutical shop. It is primarily used as disinfectant [1, 2], deodorizing [3-4], astringent [5, 6] as well as to remove iron, manganese and hydrogen sulfide from water [7]. Along with its commercial importance  $\text{KMnO}_4$  is also known for its detrimental effects like, if it is orally injected, it may lead to the death of the patient due to tissue contraction, necrosis and hepatorenal toxicity [8, 9]. The reason behind this is the oxidative injury from free radicals generated by the absorbed permanganate ion [10-12]. Genotoxicity of  $\text{KMnO}_4$

solution has been shown using a micro technique of the Ames test [13, 14]. It was also reported to cause the DNA damage in human peripheral blood lymphocytes (with a dose dependent response in single-cell gel assay (SCGA)) [15, 16]. Therefore, it is necessary to eliminate or reduce the toxic effect of  $\text{KMnO}_4$  from the environment. In order to prevent its deleterious impacts on ecosystems and public health, several extraction and recovery methods for  $\text{KMnO}_4$  have been already reported like electrochemical sensors [7], chemical reduction [17] and solvent extraction [18, 19]. The recovery methods are rather costly and time consuming. Consequently, to remove or reduce the toxic effects of  $\text{KMnO}_4$ , there is need of a method that is simple, effective, inexpensive and environmental friendly. Keeping this in mind, pentaammineazidocobalt(III) cation has been explored as an anion binder for permanganate ion in aqueous medium (green chemistry).

Moreover, if we look back the literature there are sporadic reports regarding synthesis and crystal structure determination of  $[\text{Co}(\text{NH}_3)_5\text{N}_3]^{2+}$  complex ions. The first azido complex of this cation was came into the limelight in 1934 [20] and latter on, Linhard group prepared a series of complexes containing  $[\text{Co}(\text{NH}_3)_5\text{N}_3]^{2+}$  [21, 22]. Further, there are only four reports present in literature on X-ray structure determination of complexes containing  $[\text{Co}(\text{NH}_3)_5\text{N}_3]^{2+}$  by three groups Palenik, [23] Blaurock [24] and Bala [25, 26].

Therefore, it was thought to be of interest to synthesise and study the a  $[\text{Co}(\text{NH}_3)_5\text{N}_3]^{2+}$  complex ion containing oxoanion, permanganate . This paper reports the synthesis, characterization, single crystal X-ray structure determination of  $[\text{Co}(\text{NH}_3)_5\text{N}_3](\text{MnO}_4)_2 \cdot \text{H}_2\text{O}$ . The binding properties of pentaammineazidocobalt(III) cation with permanganate anion have been determined by UV-visible titrations. The

comparative study of genotoxic effects of  $\text{KMnO}_4$ ,  $[\text{Co}(\text{NH}_3)_5\text{N}_3]\text{Cl}_2$  and  $[\text{Co}(\text{NH}_3)_5\text{N}_3](\text{MnO}_4)_2 \cdot \text{H}_2\text{O}$  have been determined using genotoxicity assay in *Allium cepa* root tip cells, which also has shown the importance to bind  $\text{MnO}_4^-$  in aqueous medium.

## 2. Materials and methods

The reagents (AR grade of Merck) were used as such without any additional purification.  $[\text{Co}(\text{NH}_3)_5\text{N}_3]\text{Cl}_2$  was prepared according to the method reported by Linhard et al. [27]. Cobalt was determined by standard method [28] and H, N was estimated microanalytically by automatic Eager 300 elemental analyzer. Solubility of the newly synthesized complex was measured at temperature  $25 \pm 2$  °C. The instrument, Shimadzu 1800 spectrophotometer was used for UV-visible spectra using quartz cuvette (water as solvent). For Infrared spectra, Varian Resolution Pro 660 FT/IR spectrophotometer was utilized as KBr pellets. XRD was recorded on a x-pert-pro PANalytical (Cu-K $\alpha$  radiation,  $\lambda = 0.15418$  nm) having angle range 5- 60°. The thermal behaviour was recorded in temperature range from 25 to 500°C (with ramp of 10 °C rate) using TGA/ DTA/ NETZSCH STA 449F1 instrument, with ramp of 10 °C.

### 2.1. Synthesis of $[\text{Co}(\text{NH}_3)_5\text{N}_3](\text{MnO}_4)_2 \cdot \text{H}_2\text{O}$

Hot (60-70 °C temperature) aqueous solution (30 mL) of pentaammineazidocobalt(III) chloride (0.50 g, 0.0019 mol) was reacted with a hot (60-70 °C temperature) aqueous solution (15 mL) of potassium permanganate (0.615g, 0.0077 mol) at room temperature. The mixture of solutions was allowed to cool slowly by keeping it overnight which resulted in formation of crystals. The crystals were filtered, air dried at room temperature. The violet coloured clear supernatant solution (after one day) gave second crop of crystals. The overall yield was 0.774 g (90 %). The melting point of the

newly synthesized complex was observed to be 415 K (dec.). Anal. Calcd. for newly synthesized complex,  $[\text{Co}(\text{NH}_3)_5\text{N}_3](\text{MnO}_4)_2 \cdot \text{H}_2\text{O}$ : Molecular weight 442.03 g/mol: Co, 13.33; N, 25.35; H, 3.88%. Found: Co, 13.32; N, 25.31; H, 3.85 %. IR ( $\text{cm}^{-1}$ ),  $\nu$  3460 (OH);  $\nu_a$  3230 ( $\text{NH}_3$ );  $\nu_s$  3194.23 ( $\text{NH}_3$ );  $\nu$  2036.90 ( $\text{N}_3$ );  $\delta_d$  1699.34 ( $\text{NH}_3$ );  $\delta_s$  1307.78 ( $\text{NH}_3$ );  $\rho_r$  833.28 ( $\text{NH}_3$ );  $\nu$  904.64 ( $\text{MnO}_4$ ). UV-vis (solution):  $\lambda_{\text{max}}$ , 303, 504, 523, 543 and 562 nm.

## 2.2. General procedure for Job's plot by UV-vis method

The stock solutions ( $1 \times 10^{-5}$  M) of receptor,  $[\text{Co}(\text{NH}_3)_5\text{N}_3]\text{Cl}_2$  and the guest,  $\text{KMnO}_4$  were prepared in aqueous medium. The absorbance in each case with different receptor (10:0)-guest (0:10) ratio but equal in volume (10 mL) was recorded. The Job's plots were drawn to find out the stoichiometries using continuous variation method at  $\lambda_{\text{max}}$  313 nm for manganate.

## 2.3. UV-visible titrations

The binding tendency of complex cation for manganate anion was determined using UV-visible titrations. The stock solutions of  $[\text{Co}(\text{NH}_3)_5\text{N}_3]\text{Cl}_2$  and  $\text{KMnO}_4$  were prepared in concentration  $1 \times 10^{-4}$  M and  $1 \times 10^{-2}$  M respectively in aqueous medium. The titration were performed by adding increments of 5  $\mu\text{L}$  solution of anion (each addition was made after 1 minute) into stock solution (2 mL) of  $[\text{Co}(\text{NH}_3)_5\text{N}_3]\text{Cl}_2$  in a quartz cuvette (optical path length 1 cm). All absorption spectra were recorded, saved and used to find the binding constant by fitting the data with the global analysis program Hypspec2014 [29, 30]

## 2.4. Crystal Structure Determination

Single-crystal diffraction data for  $[\text{Co}(\text{NH}_3)_5\text{N}_3](\text{MnO}_4)_2 \cdot \text{H}_2\text{O}$  have been collected on a Bruker AXS SMART diffractometer equipped with CCD detector. More than a

hemisphere of data was collected on each crystal over three batches of exposure using MoK $\alpha$  radiation ( $\lambda = 0.71073 \text{ \AA}$ ). A fourth set of data was measured and compared to the initial set to monitor and correct for decay, which was negligible. Data processing was performed using the program SAINT [31]. The absorption correction was done using an empirical method (SADABS) [32]. The structure was solved by the direct method and refined by the full-matrix least-squares method on all  $F^2$  data using SHELX-97 [33]. All other information regarding the refinement is also recorded in Table 1.

## 2.5. Genotoxicity of the compounds

### 2.5.1 Genotoxic potential of KMnO<sub>4</sub>, [Co(NH<sub>3</sub>)<sub>5</sub>N<sub>3</sub>]Cl<sub>2</sub> and [Co(NH<sub>3</sub>)<sub>5</sub>N<sub>3</sub>](MnO<sub>4</sub>)<sub>2</sub>·H<sub>2</sub>O

The Genotoxic potential of the compounds *viz.*, KMnO<sub>4</sub>, [Co(NH<sub>3</sub>)<sub>5</sub>N<sub>3</sub>]Cl<sub>2</sub> and [Co(NH<sub>3</sub>)<sub>5</sub>N<sub>3</sub>](MnO<sub>4</sub>)<sub>2</sub>·H<sub>2</sub>O was estimated using *Allium cepa* (onion) root chromosomal aberration assay. To evaluate genotoxicity, fresh bulbs of *Allium cepa* were peeled off and the primary roots were plucked with the help of forcep without disturbing the primordia. The onion bulbs were placed on the Couplin jars containing distilled water for germination of fresh roots. After the growth of roots to 0.5- 1 cm, they were treated with different concentrations *viz.*, 50, 100, 250 and 500 ppm of solution of all the three compounds i.e. KMnO<sub>4</sub>, [Co(NH<sub>3</sub>)<sub>5</sub>N<sub>3</sub>]Cl<sub>2</sub> and [Co(NH<sub>3</sub>)<sub>5</sub>N<sub>3</sub>](MnO<sub>4</sub>)<sub>2</sub>·H<sub>2</sub>O for 3h. The roots were then plucked and fixed in farmer's fluid (3:1:: ethanol:glacial acetic acid). The slides were prepared using squash method and were screened under microscope to score different types of aberrations. Three slides were scored for each concentration with at least 50-70 dividing cells.

## 2.5.2 Genotoxic potential of Lead Acetate

Estimation of genotoxic potential lead (0.5 ppm) was evaluated as per the protocol mentioned in section 2.5.1

## 2.5.3 Antigenotoxicity of $[\text{Co}(\text{NH}_3)_5\text{N}_3]\text{Cl}_2$ , $[\text{Co}(\text{NH}_3)_5\text{N}_3](\text{MnO}_4)_2 \cdot \text{H}_2\text{O}$ against lead

In order to see the sequential effects of newly synthesized compounds against lead induced genotoxicity, two modes of treatment i.e. pre and post were followed after germination of roots. In pretreatment, the onion roots were treated with  $[\text{Co}(\text{NH}_3)_5\text{N}_3]\text{Cl}_2$  for 3h followed by treatment with lead while in post treatment, roots were first exposed to lead solution (0.5 ppm) and then to  $[\text{Co}(\text{NH}_3)_5\text{N}_3]\text{Cl}_2$ . After treatment, the slides were prepared using standard protocol and screened for chromosomal aberrations in *Allium* root tip cells..

## 3. Results

### 3.1. Synthesis

The single pot synthetic approach was used for this synthesis of title complex. Under this approach pentaammineazidocobalt(III) chloride and potassium permanganate were reacted in 1:2 molar ratio in hot aqueous medium with the expectation of  $[\text{Co}(\text{NH}_3)_5\text{N}_3](\text{MnO}_4)_2$  complex. The violet coloured complex,  $[\text{Co}(\text{NH}_3)_5\text{N}_3](\text{MnO}_4)_2$  was formed according to expectation in addition to one lattice water molecule. The chemical composition of new cobalt(III) complex was initially confirmed by elemental analyses which corresponds to chemical formula  $[\text{Co}(\text{NH}_3)_5\text{N}_3](\text{MnO}_4)_2 \cdot \text{H}_2\text{O}$ . The methodology used for the preparation of title complex is similar as reported earlier by various groups for the preparation of  $[\text{Co}(\text{NH}_3)_5\text{N}_3]^{2+}$  containing complexes [20-26].

Solubility product

The newly synthesized complex is insoluble in organic solvent ( $\text{CCl}_4$ ,  $\text{CHCl}_3$ ) but soluble in inorganic solvent (DMSO, MeCN) indicating the ionic behaviour. Solubility of ionic complex in water differs to a great extent and on the basis of solubility criterion, the ionic complexes are classified into three categories (a) solubility  $> 0.1$  M (soluble) (b) solubility between 0.01 and 0.1 M (slightly soluble) (c) solubility  $< 0.01$  M (sparingly soluble). The solubility product,  $K_{sp}$  of new cobalt(III) complex is  $5.41 \times 10^{-5}$  at  $25 \pm 2$  °C, indicating its slight solubility in water. The order of solubility was observed as:  $\text{KMnO}_4 > [\text{Co}(\text{NH}_3)_5\text{N}_3]\text{Cl}_2 > [\text{Co}(\text{NH}_3)_5](\text{MnO}_4)_2 \cdot \text{H}_2\text{O}$ .

### 3.2. UV/Visible spectrum

All the UV/Visible spectra were recorded in water. The two transitions approximately at 515 ( $^1\text{A}_{1g} \rightarrow \text{T}_{1g}$ ) and 302 nm ( $^1\text{A}_{1g} \rightarrow ^1\text{T}_{2g}$ ) were described [25-27] for pentaammineazidocobalt(III) cation containing complexes, producing the familiar dark violet colour. For  $[\text{Co}(\text{NH}_3)_5\text{N}_3]\text{Cl}_2$  these transitions were observed at 518 and 299 nm (See Figure 1). However for  $\text{KMnO}_4$ , five peaks were observed at 509, 527, 547, 569 and 313 nm along with one shoulder around 354 nm (see Figure 1) although it is  $d^0$  system, Mn(+7). These peaks are observed due to ligand to metal charge transfer bands (LMCT) i.e, an O lone-pair electron is promoted into a low-lying empty e orbital of metal. But for  $[\text{Co}(\text{NH}_3)_5\text{N}_3](\text{MnO}_4)_2 \cdot \text{H}_2\text{O}$ , the maxima were observed at 303, 504, 523, 543 and 562 nm (See Figure 1). The disappearance of peaks at 313 and 515 nm of  $\text{MnO}_4^-$  and  $[\text{Co}(\text{NH}_3)_5\text{N}_3]^{2+}$  respectively may be due to overlapping of d-d transitions of Co(III) with charge transfer bands of  $\text{MnO}_4^-$  i.e., 313 nm of  $\text{MnO}_4^-$  (charge transfer band) merged with 299 nm of Co(III) cation (d-d transition) and 518 nm of Co(III) cation (d-d transition) merged with 527 nm  $\text{MnO}_4^-$  (charge transfer band).



### 3.3. Jobs Plot and UV/Visible titrations

After taking the UV-visible spectra of complex cation and anion (Figure 2 a), the stoichiometry was determined by Job's plot (using continuous variation method) at different  $\lambda_{\max}$  313 nm. Jobs plot is plotted between  $\Delta A * XR$  or  $XG$  (mole fraction of receptor or guest) (along  $y$ -axis) and  $XR$  or  $XG$  (along  $x$ -axis) in the mixtures where the total concentrations of receptor and guest remain constant. It is used to identify the stoichiometry of the complex. The maximum were observed at 0.35 mole fraction with respect to receptor respectively, which implied the stoichiometry to be 1:2 (see Figure 2 b).

For investigating the binding properties of  $[\text{Co}(\text{NH}_3)_5\text{N}_3]^{2+}$  for permanganate anion ( $\text{MnO}_4^-$ ), titration experiments were performed according to the procedure given in the experimental section. After constant additions of  $\text{KMnO}_4$  in receptor (R) a gradual red shift (bathochromic shift) is observed from absorption maxima 299 to 306 nm along with hyperchromic shift in all the absorption maxima (which were observed at 507, 525, 545 and 564 nm, See Figure 3). The disappearance of peaks at 313 and 515 nm of  $\text{MnO}_4^-$  and  $[\text{Co}(\text{NH}_3)_5\text{N}_3]^{2+}$  respectively and 7 nm red shift in the presence of permanganate anion could result in the interaction between receptor and anion. Through the spectral fitting of titration data the  $\log \beta$  value was observed at  $8.8128 \pm 0.02$  with the formation stoichiometry 1:2 for  $\text{MnO}_4^-$ . This stoichiometry was also matched with the stoichiometry obtained from the Job's plot titrations (Figure 2 b).

### 3.4. Infrared spectrum

The infrared spectrum of  $[\text{Co}(\text{NH}_3)_5\text{N}_3](\text{MnO}_4)_2 \cdot \text{H}_2\text{O}$  has been recorded in the range 400 to 4000  $\text{cm}^{-1}$  and interpretations have been made on the basis of earlier reported literature [25, 26, 34]. In new cobalt(III) complex, the stretching vibration frequencies

were lower for the coordinated  $\text{NH}_3$  molecules than those of the free  $\text{NH}_3$ . This lowering might be due to the formation of N-H...O type of hydrogen bonds which weaken the N-H bonds. It has been observed that the rocking vibrations ( $\rho_r$ ), symmetric deformation ( $\delta_s$ ), degenerate deformation ( $\delta_d$ ), and antisymmetric ( $\nu_{as}$ ) and symmetric ( $\nu_s$ ) stretch appeared in the regions of 800-900, 1370-1200, 1650-1550, and 3400-3000  $\text{cm}^{-1}$  respectively [25] for  $[\text{Co}(\text{NH}_3)_5\text{N}_3]\text{Cl}_2$  which was comparable with  $[\text{Co}(\text{NH}_3)_5\text{N}_3](\text{MnO}_4)_2 \cdot \text{H}_2\text{O}$ . For ionic  $\text{MnO}_4^-$  a sharp band was observed at 904  $\text{cm}^{-1}$  for  $[\text{Co}(\text{NH}_3)_5\text{N}_3](\text{MnO}_4)_2 \cdot \text{H}_2\text{O}$  which is comparable with the band observed in case of potassium permanganate i.e., 902  $\text{cm}^{-1}$  [34].

### 3.5. TG/DT/DTG Analysis

Thermal stability of title complex was examined between 20 and 800 °C under nitrogen flow (Figure 4). The decomposition of complex started with the loss of water and azide in two steps, one at 117 °C and other at 125 °C. The complete loss (water and azide) occurs at 159 °C (13.6 %) followed by loss of ammonia and decomposition of  $\text{MnO}_4^-$  up to temperature 183 °C. Both these decomposition steps were exothermic in nature (See Figure 4). After that not much change in weight loss was observed.

### 3.6. Single crystal X-ray diffraction (SCXRD)

The X-ray crystal structure of the  $[\text{Co}(\text{NH}_3)_5\text{N}_3](\text{MnO}_4)_2 \cdot \text{H}_2\text{O}$  was unambiguously determined by single crystal X-ray crystallography. The crystal structure conclusively established the existence of single complex of composition,  $[\text{Co}(\text{NH}_3)_5\text{N}_3](\text{MnO}_4)_2 \cdot \text{H}_2\text{O}$  and also ruled out the possibility of a double salt and mixture of salts. Furthermore, this study revealed for the first time that it is an ionic complex which contains discrete ions,  $[\text{Co}(\text{NH}_3)_5\text{N}_3]^{2+}$  and two  $\text{MnO}_4^-$  in addition to one lattice water molecule in the solid

state. The numbering scheme and ORTEP diagram of  $[\text{Co}(\text{NH}_3)_5\text{N}_3](\text{MnO}_4)_2 \cdot \text{H}_2\text{O}$  is shown in Figure 5a.

In  $[\text{Co}(\text{NH}_3)_5\text{N}_3]^{2+}$ , the cobalt(III) metal ion is surrounded by six nitrogen atoms originating from five coordinating ammonia molecules and one from azide molecule resulting in a nearly octahedral geometry. The Co–NH<sub>3</sub> bond distances are in the range 1.958(4) - 1.981(5) Å while cis H<sub>3</sub>N–Co–NH<sub>3</sub> bond angles are in the range 89.16(18) - 92.1(2)° and trans H<sub>3</sub>N–Co–NH<sub>3</sub> bond angles are in the range 177.4(2) - 178.86(18)°. The Co–N<sub>3</sub> bond distance is 1.955(5) Å, while cis H<sub>3</sub>N–Co–N<sub>3</sub> and trans H<sub>3</sub>N–Co–N<sub>3</sub> bond angles are in the range 86.1(2) - 91.3(2)° and 177.4(2) - 178.86(18)° respectively. This study showed that octahedron is slightly distorted. The bonding parameters of  $[\text{Co}(\text{NH}_3)_5\text{N}_3](\text{MnO}_4)_2 \cdot \text{H}_2\text{O}$  are also in accordance with the former reported  $[\text{Co}(\text{NH}_3)_5\text{N}_3]^{2+}$  complex ion [23-26]. The selected bond angles and bond lengths are listed in Table 2. In the pentaammineazidocobalt(III) azide, the average Co–NH<sub>3</sub> bond distance is 1.968 Å and average bond angles cis and trans H<sub>3</sub>N–Co–NH<sub>3</sub> are 90.7° and 179.8° respectively.

In the  $\text{MnO}_4^{2-}$ , the Mn–O bond distances are in the range 1.579(5) - 1.620(4) Å. The O–Mn–O bond angles are in the range 108.3(2) - 111.7(3)°. In literature, average Mn–O bond distance is 1.605 Å and average O–Mn–O bond angle is 109.5° for permanganate anion [35].

In the crystal lattice of title complex, supramolecular architecture is also formed (See Table 3). It is formed by intermolecular hydrogen bonding between: 1) cation and anion (N–H(NH<sub>3</sub>)...O (MnO<sub>4</sub><sup>-</sup>)), 2) solvent molecule (water) and cation (H–O (water)...H–N (cation)) and 3) solvent molecule (water) and anion (H–O–H (water)...O–Mn(anion)). The hydrogen bonding parameters are given in Table 3. This supramolecular

architecture stabilizes the crystal lattice along with electrostatic forces of attractions between cations and anions. All kinds of hydrogen bonding interactions are shown in Figure 5b.

### **3.7. Powder X-ray diffraction (PXRD)**

The simulated PXRD pattern of title compound is given in Figure 6 (a). The simulated XRD pattern was compared with the SCXRD pattern obtained from the cif file (Figure 6(b)) of the compound and they are similar to one another. This indicates that SCXRD pattern obtained from cif file have same crystalline phase with respect to their bulk materials.

### **3.8. Genotoxic potential**

#### **3.8.1 Genotoxic potential of $\text{KMnO}_4$ , $[\text{Co}(\text{NH}_3)_5\text{N}_3]\text{Cl}_2$ and $[\text{Co}(\text{NH}_3)_5\text{N}_3](\text{MnO}_4)_2 \cdot \text{H}_2\text{O}$ (Table 4)**

$\text{KMnO}_4$  was analyzed for its genotoxic potential and it was observed that its treatment on *Allium cepa* root tip cells resulted in physiological aberrations at all the concentrations (12, 25, 50 125 and 250 ppm) and total percent aberrant cells ranged from 64.37 to 80.48 %. Ramsdorff et al. 2009 [15] has also reported the genotoxic effects of  $\text{KMnO}_4$  in acidic conditions with a dose-response relationship as determined by Single Cell Gell Assay (SCGA). The authors reported that the conversion of  $\text{MnO}_4^-$  to  $\text{Mn}^{2+}$  resulted in the DNA damage in human lymphocytes. However, in our study we observe that  $\text{KMnO}_4$  did not induced only clastogenic aberrations.  $[\text{Co}(\text{NH}_3)_5\text{N}_3]\text{Cl}_2$  has induced both physiological and clastogenic aberrations at 50, 100, 250 and 500 ppm) and it observed that the genotoxic potential of  $[\text{Co}(\text{NH}_3)_5\text{N}_3]\text{Cl}_2$  was less as compared to  $\text{KMnO}_4$ .

However it was interesting to note that when the newly synthesized complex was evaluated  $[\text{Co}(\text{NH}_3)_5\text{N}_3](\text{MnO}_4)_2 \cdot \text{H}_2\text{O}$  for its genotoxic potential at all concentration (at 25, 50, 100, 250 and 500 ppm), it induced almost half the number of chromosomal aberrations when compared to that of treatment with  $\text{KMnO}_4$ . The probable reason behind this can be the less toxic behavior of newly synthesized complex,  $[\text{Co}(\text{NH}_3)_5\text{N}_3](\text{MnO}_4)_2 \cdot \text{H}_2\text{O}$  due to the fact of non availability of  $\text{Mn}^{2+}$  ions in the solution.

### 3.8.2 Genotoxic potential of Lead Acetate

It was observed that lead acetate (0.5 ppm) has induced 46.83 % total aberrant cells comprising of 40.50 % physiological and 6.33 % clastogenic aberrations in *Allium cepa* root tip cells. The physiological aberrations included delayed anaphase/s (Da), stickiness (St), spindle inhibition (Sp), laggard/s (Lg) vagrant/s (Vg), abnormal anaphase/s (Aa) and abnormal metaphase/s (Am), while chromatin Bridge/s (Bg) and chromosomal break/s (Bk) constituted the clastogenic aberrations [Figure 7]. The genotoxicity of lead using various bioassays has been well documented [36-39]. To evaluate if the complexes,  $[\text{Co}(\text{NH}_3)_5\text{N}_3]\text{Cl}_2$  and  $[\text{Co}(\text{NH}_3)_5\text{N}_3](\text{MnO}_4)_2 \cdot \text{H}_2\text{O}$  could reduce the genotoxic potential of other carcinogenic chemicals (Table 5)

The study was further carried out to explore the genotoxic potential of  $[\text{Co}(\text{NH}_3)_5\text{N}_3]\text{Cl}_2$  and  $[\text{Co}(\text{NH}_3)_5\text{N}_3](\text{MnO}_4)_2 \cdot \text{H}_2\text{O}$  combined with lead acetate using pre and post- treatments. Although the newly synthesized complex  $[\text{Co}(\text{NH}_3)_5\text{N}_3](\text{MnO}_4)_2 \cdot \text{H}_2\text{O}$  showed less genotoxic potential as compared to  $\text{KMnO}_4$  but it did not reduce the effects of lead acetate when treated in combination with lead acetate during pre and post-treatments. On the other hand, the complex  $[\text{Co}(\text{NH}_3)_5\text{N}_3]\text{Cl}_2$  reduced the toxicity of lead acetate when treated in combination with

lead acetate during pre and post treatments. Thus, it can be concluded that the complex  $[\text{Co}(\text{NH}_3)_5\text{N}_3]\text{Cl}_2$  can be explored as a potential anion receptor for the extraction of environmentally hazardous chemicals like lead.

#### **4. Conclusion**

Lastly, it is concluded that crystals of  $[\text{Co}(\text{NH}_3)_5\text{N}_3](\text{MnO}_4)_2\cdot\text{H}_2\text{O}$  can be formed by reacting  $\text{KMnO}_4$  with  $[\text{Co}(\text{NH}_3)_5\text{N}_3]\text{Cl}_2$  in aqueous medium. The X-ray crystallographic study of  $[\text{Co}(\text{NH}_3)_5\text{N}_3](\text{MnO}_4)_2\cdot\text{H}_2\text{O}$  shows the presence of discrete ions: one cation, two anion along with one water of crystallization in solid state. The binding ability of cation,  $[\text{Co}(\text{NH}_3)_5\text{N}_3]^{2+}$  towards anion shows that ions remain intact in the aqueous medium also. Further, the genotoxic effects of potassium  $\text{KMnO}_4$ ,  $[\text{Co}(\text{NH}_3)_5\text{N}_3]\text{Cl}_2$  and  $[\text{Co}(\text{NH}_3)_5\text{N}_3](\text{MnO}_4)_2\cdot\text{H}_2\text{O}$  have been determined using *Allium cepa* root chromosomal aberration assay. The relative genotoxicity of these compounds has following decreasing order:  $\text{KMnO}_4 > [\text{Co}(\text{NH}_3)_5\text{N}_3](\text{MnO}_4)_2\cdot\text{H}_2\text{O} > [\text{Co}(\text{NH}_3)_5\text{N}_3]\text{Cl}_2$ . This order shows the significance to bind the  $\text{MnO}_4^-$  with  $[\text{Co}(\text{NH}_3)_5\text{N}_3]^{2+}$  under the conditions of environmental prevalence of it.

#### **Acknowledgement**

We thank the CSIR and UGC, New Delhi, India for their financial support under Grant No. 01(2517)/11/EMR-II dated 12.02.2011 and Grant No.- 41-285/2012 (SR) dated 13-07-2012 respectively. I am also thankful to Prof. P. Venugopalan, Department of Chemistry, Panjab University, Chandigarh, India for solving the structure. I am also thankful to Dr. Jatinder Kaur for doing genotoxic studies of coordination compounds.

#### **Supplementary material**

Full lists of crystallographic data are available from the authors upon request. Crystallographic data for the structural analysis of the title compound has also been

deposited at the FIZ, 76344 Eggenstein-Leopoldshafen (Germany), having CSD number 426476 (tel.: (49) 7247-808-205; fax: (49) 7247-808-666; E-mail: [crysdata@fiz-karlsruhe.de](mailto:crysdata@fiz-karlsruhe.de)).

### **Declaration of interests**

The authors declare that they have no known competing financial interests or personal relationships that could have appeared to influence the work reported in this paper.

### **References**

1. Mohammed HH, Arias CR. Potassium permanganate elicits a shift of the external fish microbiome and increases host susceptibility to columnaris disease. *Veterinary Research* 2015; 46 (82): 1-13. doi: 10.1186/s13567-015-0215-y
2. McCrory DF, Hobbs P. Additives to Reduce Ammonia and Odor Emissions from Livestock Wastes: A Review. *Journal of Environmental Quality* 2001; 30 (2): 345-355. doi: 10.2134/jeq2001.302345x
3. Yamakawa T. Deodorizing activity and effect of potassium permanganate, *Fragrance Journal*. *Fragrance J* 1985; 13 (3): 54-55.
4. Zheng M, Peng T, Zheng J, Faming Zhuanli Shenqing CN 106621770 A 20170510; 2017 (patent).
5. Hobbs MS, Grippo RS, Farris JL, Griffin RR, Harding LL. Comparative acute toxicity of potassium permanganate to nontarget aquatic organisms. *Environmental Toxicology and Chemistry* 2006; 25 (11): 3046-3052. doi: 10.1897/05-453R2.1
6. Zahran E, Risha E. Protective role of adjuvant and potassium permanganate on oxidative stress response of Nile tilapia (*Oreochromis niloticus*) challenged with *Saprolegnia ferax*. *SpringerPlus* 2013; 2 (94): 1-13. doi: 10.1186/2193-1801-2-94

7. Faridbod F, Ganjali MR, Hosseini M, Norouzi P. Permanganate Selective Nano-composite Electrode International Journal of Electrochemical Science 2012; 7 (3): 1927-1936.
8. Johnson T B, Cassidy D D. Unintentional Ingestion of Potassium Permanganate. Pediatric Emergency Care 2004; 20 (3): 185-187. doi: 10.1097/01.pec.0000117926.65522.33
9. Korkut E, Saritas A, Aydin Y, Korkut S, Kandis H et al. Suicidal ingestion of potassium permanganate. World Journal Emergncy Medicine 2013; 4 (1): 73-74. doi: 10.5847/wjem.j.issn.1920-8642.2013.01.014
10. Young RJ, Critchley JA, Young KK, Freebairn RC, Reynolds AP et al. Fatal acute hepatorenal failure following potassium permanganate ingestion. Human Experimental Toxicology 1996; 15 (3): 259-261. doi: 10.1177/096032719601500313
11. França JG, Ranzani-Paiva MJT, Lombardi JV, Carvalho S de, Filipak-Neto F et al. Toxic effect of potassium permanganate on *Oreochromis niloticus* based on hematological parameters and biomarkers of oxidative stress. International Journal of Fisheries and Aquaculture 2013; 5 (1): 1-6. doi: 10.5897/IJFA12.050
12. Ghelichpour M, Eagderi S. Toxicological effects of potassium permanganate on two different sizes of angelfish (*Pterophyllum scalare*). Global Veterinaria 2012; 9 (2): 140-143. doi: 10.5829/idosi.gv.2012.9.2.6469
13. Méo MD, Laget M, Castegnaro M. Genotoxic activity of potassium permanganate in acidic solutions. Mutation Research, Genetic Toxicology Testing 1991; 260 (3): 295-306. doi: 10.1016/0165-1218(91)90038-n



14. Mehrabian S, Shirkhodaei E. Modulation of Mutagenicity of Various Mutagens by Shrimp Flesh and Skin Extracts in Salmonella Test. *Pakistan Journal of Biological Sciences* 2006; 9 (4): 598-600.
15. Ramsdorf WA, Ferraro MVM, Oliveira-Ribeiro CA, Costa JRM, Cestari MM. Genotoxic evaluation of different doses of inorganic lead (PbII) in *Hoplias malabaricus*. *Environ Monit Assess* 2009; 158: 77-85. doi: 10.1007/s10661-008-0566-1
16. Koizume S, Inoue H, Kamiya H, Ohtsuka E. Neighboring base damage induced by permanganate oxidation of 8-oxoguanine in DNA. *Nucleic Acids Research* 1998; 26 (15): 3599-3607. doi: 10.1093/nar/26.15.3599
17. Okitsu K, Nishimura R. Sonochemical reduction method for controlled synthesis of metal nanoparticles in aqueous solutions. *Proceedings of 20<sup>th</sup> international Congress on Acoustics, ICA Sydney, Australia; 2010, pp. 1-3.*
18. Kostova D, Kamburova M. Solvent extraction of manganese (VII) with a new analytical reagent *Chemie* 2008; 19: 27-32.
19. Kudo Y, Harashima K, Katsuta S, Takeda Y. Solvent extraction of sodium permanganate by mono-benzo 3m-crown-m ethers (m = 5, 6) into 1,2-dichloroethane and nitrobenzene: a method which analyzes the extraction system with the polar diluents. *International Journal of Chemistry* 2011; 3 (1): 99-107. doi: 10.5539/ijc.v3n1p99
20. Strecker W, Oxenius H. Über die Einführung der Azidgruppe in Komplexsalzen des Kobalts. *Zeitschrift für anorganische und allgemeine Chemie* 1934; 218: 151-160. doi: 10.1002/zaac.19342180206

21. Linhard M, Flygare H. Über Komplexverbindungen. IV. Azidopentammincobalt(III)-komplexe. Zeitschrift für anorganische und allgemeine Chemie 1950; 262: 328-343. doi: 10.1002/zaac.19502620606
22. Linhard M, Weigel M. Über Komplexverbindungen. XI Lichtabsorption von Azidocobalt-amminen. Zeitschrift für anorganische und allgemeine Chemie 1952; 267: 121-130. doi: 10.1002/zaac.19522670113
23. Palenik G J. The Structure of Coordination Compounds I. The Crystal and molecular structure of azidopentamminecobalt(III) azide. Acta Crystallographica 1964; 17: 360-367. doi: 10.1107/S0365110X64000858
24. Blaurock S, Edelmann FT. Crystal Structures of Energetic Compounds. I. Safe Small-Scale Preparation and X-Ray Structure determination of the high-energy cobalt(III) complex  $[\text{Co}(\text{NH}_3)_5\text{N}_3](\text{N}_3)_2$ . Journal of Chemical Crystallography 2009; 39 (9): 646-649. doi: 10.1007/s10870-009-9548-6
25. Bala R, Kaur N, Kim J. The first complex of azidopentaamminecobalt(III) containing organic anion: Synthesis, characterization and X-ray structure determination of azidopentaamminecobalt(III) *p*-nitrobenzoate dihydrate. Journal of Molecular Structure 2011; 1003 (1-3): 47-51. doi: 10.1016/j.molstruc.2011.07.016
26. Bala R, Behal J, Shah NA, Rathod KN, Prakash V et al. Sonochemical synthesis, characterization, thermal and semiconducting behavior of nano-sized azidopentaamminecobalt(III) complexes containing anion,  $\text{CrO}_4^{2-}$  or  $\text{Cr}_2\text{O}_7^{2-}$ . Ultrasonics Sonochemistry 2018; 41: 172-180 doi: 10.1016/j.ultsonch.2017.09.038
27. Linhard M, Weigel M. Über Komplexverbindungen. VI. Triazido-triammin-kobalt Mit 1 Abbildung. Zeitschrift für anorganische und allgemeine Chemie 1950; 263 (5-6): 245-252. doi: 10.1002/zaac.19502630505

28. Vogel AI. A Text Book of Quantitative Inorganic Analysis, 3<sup>rd</sup> ed Longman, London, 1961.
29. Gans P, Sabatini A, Vacca A. Investigation of equilibria in solution. Determination of equilibrium constants with the HYPERQUAD suite of programs. *Talanta* 1996; 43 (10): 1739-1953 doi: 10.1016/0039-9140(96)01958-3
30. [www.hyperquadcouk/HypSpechtml](http://www.hyperquadcouk/HypSpechtml)
31. SAINT-Plus, Version 602, Bruker Analytical X-ray System, Madison, WI; 1999.
32. G M Sheldrick, SADABS University of Göttingen, Germany, 1996.
33. Sheldrick GM. A short history of SHELX. *Acta Crystallographica Section A* 2008; 64 (1): 112-122. doi: 10.1107/S0108767307043930
34. Nakamoto K. Infrared and Raman Spectra of Inorganic and Coordination Compounds 5<sup>th</sup> ed, John Wiley and Sons, New York, 1997.
35. Palenik GJ. Crystal structure of potassium permanganate. *Inorganic Chemistry* 1967; 6 (3): 503-507. doi: 10.1021/ic50049a015
36. Ibrahim NM, Eweis EA, El-Beltagi HS, Abdel-Mobdy YE. Effect of lead acetate toxicity on experimental male albino rat. *Asian Pacific Journal of Tropical Biomedicine* 2012; 2 (1): 41-46. doi: 10.1016/S2221-1691(11)60187-1
37. Stone CL, Mahaffey KR. A rapid bioassay system for lead using young Japanese quail. *Journal of Environmental Pathology and Toxicology* 1979; 2 (3): 767-779.
38. Vahideh G, Nasser MS, Ereshteh G, Seddiq MM, Elham M et al. The effect of lead toxicity on embryonic development and early larval growth of the echinometra mathaei sea urchin (Persian Gulf), morphologic and morphometric studies. *Annals of Biological Research* 2012; 3 (7): 3321-3327.

39. Alkahemal-Balawi HF, Ahmad Z, Al-Akel AS, Al-Misned F, Suliman EM et al. Toxicity bioassay of lead acetate and effects of its sub-lethal exposure on growth, haematological parameters and reproduction in clarias gariepinus African Journal of Biotechnology. 2011; 10 (53): 11039-11047. doi: 10.5897/ajb11.1463

**Table 1** Crystal structure refinement data of  $[\text{Co}(\text{NH}_3)_5\text{N}_3](\text{MnO}_4)_2 \cdot \text{H}_2\text{O}$

Empirical formula	H17 Co Mn2 N8 O9 (Figure 5)
Formula weight	442.03
Temperature (K)	293(2)
Crystal system, space group	Monoclinic, Cc
Unit cell dimensions	$a = 9.4996(15) \text{ \AA}$ $b = 12.110(2) \text{ \AA}$ $c = 12.704(2) \text{ \AA}$ $\beta = 107.733(9)^\circ$
Volume ( $\text{\AA}^3$ )	1392.0(4)
Z, calculated density ( $\text{g/cm}^3$ )	4, 2.109
Absorption coefficient ( $\text{mm}^{-1}$ )	3.020
F(000)	888
$\theta$ range for data collection ( $^\circ$ )	2.81- 38.83
Index ranges	$-16 \leq h \leq 16$ , $-17 \leq k \leq 21$ , $-22 \leq l \leq 16$
Reflections collected	16219
Independent reflections	6188 [ $R_{\text{int}} = 0.0463$ ]
Data/restraints/parameters	6188/ 2/181
Goodness-of-fit on $F^2$ , (S)	1.010
Final R indices, 288 reflections [ $I > 2\sigma(I)$ ]	$R1=0.0439$ , $wR2 = 0.0826$
R indices (all data)	$R1= 0.0865$ , $wR2= 0.0967$

**Table 2** Bonding parameters, lengths (Å) and angles (°)

Co1-N1	1.967(4)	Mn1-O1	1.616(4)
Co1-N2	1.966(4)	Mn1-O2	1.579(5)
Co1-N3	1.958(4)	Mn1-O3	1.606(4)
Co1-N4	1.965(4)	Mn1-O4	1.598(4)
Co1-N5	1.981(5)	Mn2-O5	1.591(5)
Co1-N6	1.955(5)	Mn2-O6	1.602(4)
N6-N7	1.187(5)	Mn2-O7	1.620(4)
N7-N8	1.159(5)	Mn2-O8	1.586(5)
N1-Co1-N5	92.1(2)	N7-N6-Co1	121.5(3)
N2-Co1-N1	89.80(10)	N8-N7-N6	177.0(5)
N2-Co1-N5	90.2(2)	O2-Mn1-O1	109.9(3)
N3-Co1-N1	177.4(2)	O2-Mn1-O3	109.6(3)
N3-Co1-N2	90.11(17)	O2-Mn1-O4	108.4(3)
N3-Co1-N4	90.92(11)	O3-Mn1-O1	109.5(3)
N3-Co1-N5	90.4(2)	O4-Mn1-O1	109.3(3)
N4-Co1-N1	89.16(18)	O4-Mn1-O3	110.2(3)
N4-Co1-N2	178.86(18)	O5-Mn2-O6	111.7(3)
N4-Co1-N5	90.3(2)	O5-Mn2-O7	109.9(3)
N6-Co1-N1	86.1(2)	O6-Mn2-O7	108.3(2)
N6-Co1-N2	89.56(19)	O8-Mn2-O5	108.3(3)
N6-Co1-N3	91.3(2)	O8-Mn2-O6	108.6(3)
N6-Co1-N4	89.92(19)	O8-Mn2-O6	108.6(3)

**Table 3.** Hydrogen bonding parameters (Å, °)

D-H...A	D - H	H...A	D...A	<D - H... A	Symmetry operations
N1-H1A...O(8)	0.89	2.36	3.149(7)	148	i
N1-H1B...O(5)	0.89	2.15	3.030(8)	170	ii
N1-H1C...O(6)	0.89	2.40	3.251(7)	160	iii
N2-H2B...O(7)	0.89	2.23	3.095(6)	164	iii
N2-H2C...O(5)	0.89	2.30	3.168(7)	164	i
N3-H3A...O(4)	0.89	2.50	2.966(8)	113'	iv
N3-H3B...O(9)	0.89	2.16	2.931(6)	144	i
N3-H3C...O(7)	0.89	2.10	2.971(7)	168	iv
N4-H4A...O(3)	0.89	2.54	2.934(6)	107	iv
N4-H4A...N(8)	0.89	2.28	3.147(7)	163'	vii
N4-H4B...O(6)	0.89	2.19	3.039(7)	159	iii
N4-H4C...O(2)	0.89	2.33	3.002(7)	133	vi
N4-H4C...O(9)	0.89	2.24	2.984(6)	141'	v
N5-H5A...N(8)	0.89	2.54	3.402(7)	162	vii
N5-H5C...O(6)	0.89	2.48	3.257(7)	146	ii
O9-H9A...O(2)	0.98	2.11	3.021(8)	154'	v

i = x, -y, 1/2+z; ii = -1/2+x, -1/2+y, z; iii = -1/2+x, 1/2-y, 1/2+z; iv = 1/2+x, 1/2-y, 1/2+z; v = x, 1-y, 1/2+z; vi = x, y, 1+z, vii = -1/2+x, 1/2-y, -1/2+z

1 **Table 4.** Genotoxic potential of potassium permanganate (KMnO<sub>4</sub>), azidopentaaminecobalt(III) chloride ([Co(NH<sub>3</sub>)<sub>5</sub>N<sub>3</sub>]Cl<sub>2</sub>) and  
 2 azidopentaaminecobalt(III) permanganate [Co(NH<sub>3</sub>)<sub>5</sub>N<sub>3</sub>](MnO<sub>4</sub>)<sub>2</sub>.H<sub>2</sub>O in *Allium cepa* root chromosomal aberrations assay  
 3

Treatment	Concentration (ppm)	TC	TNDC	Number of cells with														TNAC (PA+CA)	
				Physiological aberrations (PA)										Clastogenic aberrations (CA)				No.	%
				Da	St	Si	Lg	Vg	Aa	Am	Total PA	% PA	Bg	Bk	Total CA	% CA			
-ve control (distilled water)	0	3333	150	2	2	-	1	-	2	1	12	8.00	-	1	1	1.13	13	8.66	
+ve control Pb (0.5 ppm)	0.5	3064	158	11	39	9	-	-	5	-	64	40.50	8	2	10	6.33	74	46.83	
KMnO <sub>4</sub>	12	2350	160	1	22	47	-	-	26	7	103	64.37	-	-	-	-	103	64.37	
	25	2239	154	2	20	48	-	-	23	20	113	73.37	-	-	-	-	113	73.37	
	50	2205	156	2	26	47	-	-	36	14	125	80.12	-	-	-	-	125	80.12	
	125	2634	161	5	22	48	-	-	30	18	123	76.39	-	-	-	-	123	76.39	
	250	2275	164	6	38	58	-	-	22	08	132	80.48	-	-	-	-	132	80.48	
[Co(NH <sub>3</sub> ) <sub>5</sub> N <sub>3</sub> ]Cl <sub>2</sub>	50	2218	156	5	3	6	-	-	2	7	23	14.74	-	-	-	-	23	14.74	
	100	1556	154	-	1	5	1	-	5	6	18	11.68	-	-	-	-	18	11.68	
	250	3310	168	8	27	2	-	2	1	5	45	26.78	3	-	3	1.78	48	28.57	
	500	2490	150	2	27	5	-	1	-	6	41	27.33	1	-	1	0.66	42	28.00	
[Co(NH <sub>3</sub> ) <sub>5</sub> N <sub>3</sub> ](MnO <sub>4</sub> ) <sub>2</sub> .H <sub>2</sub> O	50	1854	155	1	9	28	-	-	17	7	62	40.00	1	-	1	0.6	63	40.64	
	100	2387	156	1	20	27	-	-	17	9	75	48.07	-	-	-	-	75	48.07	
	250	2527	158	1	15	20	-	-	19	12	67	42.40	5	-	5	3.16	72	45.57	
	500	2581	155	1	25	23	-	-	32	10	91	58.70	-	-	-	-	91	58.70	

4 TC-Total Cells, TNAC-Total number of aberrant cells, -ve control-negative control, +ve control-positive control, Da- Delayed anaphase, Bk-Chromosomal break, St-  
 5 Sticky, Si-spindle inhibition, Aa-Abnormal anaphase, Am-Abnormal metaphase, Lg-laggard/s, Vg-vagrant/s, Bg- Chromatin bridge

1 **Table 5.** Genotoxic Potential of azidopentaaminecobalt(III) chloride ( $[\text{Co}(\text{NH}_3)_5\text{N}_3]\text{Cl}_2$ ) and azidopentaaminecobalt(III) permanganate  
 2 monohydrate ( $[\text{Co}(\text{NH}_3)_5\text{N}_3](\text{MnO}_4)_2 \cdot \text{H}_2\text{O}$ ) against lead induced genotoxicity in *Allium cepa* root chromosomal aberrations assay

3

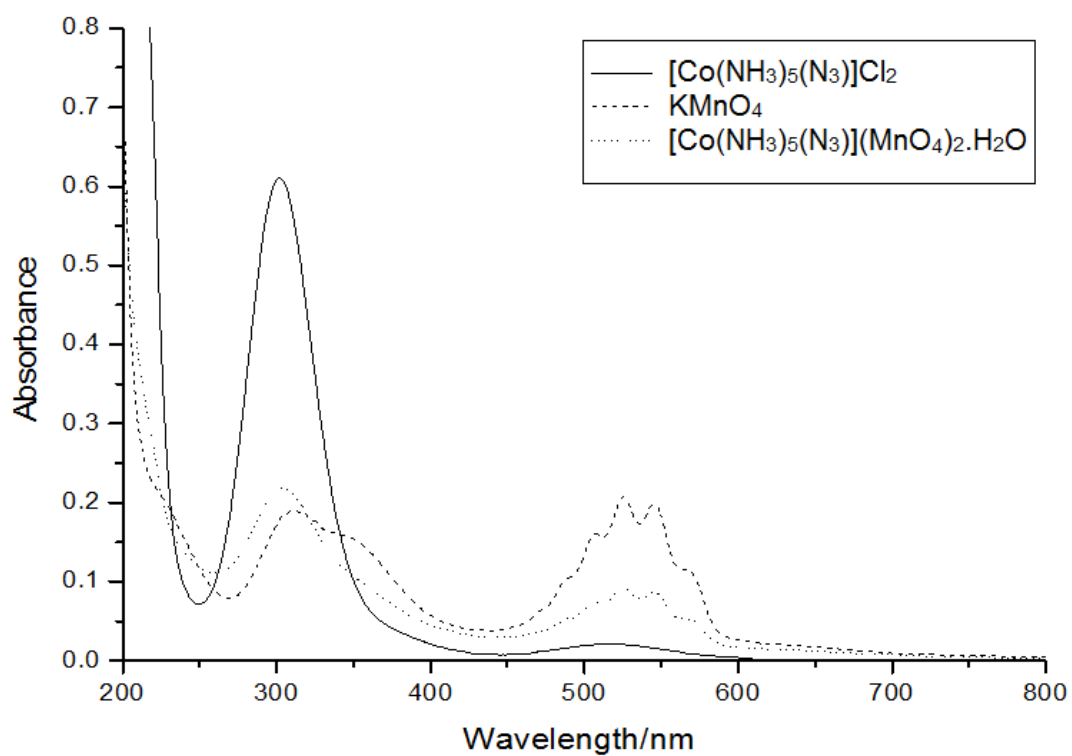
Treatment	Concentration (ppm)	TC	TNDC	Number of cells with														TNAC (PA+CA)	
				Physiological aberrations (PA)										Clastogenic aberrations (CA)				No.	%
				Da	St	Si	Lg	Vg	Aa	Am	Total PA	% PA	Bg	Bk	Total CA	% CA			
$[\text{Co}(\text{NH}_3)_5\text{N}_3]\text{Cl}_2$	(Pre-treatment)	50	1551	163	2	2	62	-	-	6	4	76	46.62	1	-	1	0.6	77	35.05
		100	2652	158	-	07	12	-	-	3	10	32	20.25	-	-	-	-	32	20.25
		250	2842	156	-	23	14	-	-	6	07	50	32.05	-	-	-	-	50	22.00
		500	2093	156	-	13	08	-	-	5	5	31	19.87	2	-	2	0.13	33	21.15
	(Post-treatment)	50	2431	164	-	11	13	1	-	5	1	31	18.90	2	-	2	1.21	33	20.12
		100	3022	156	2	08	26	-	-	2	0	39	25.00	-	-	-	-	39	25.00
		250	1650	156	1	14	12	-	-	6	2	35	22.43	3	-	3	1.92	38	24.35
		500	2386	159	5	14	33	-	-	5	2	59	36.87	4	-	4	2.50	63	39.62
$[\text{Co}(\text{NH}_3)_5\text{N}_3](\text{MnO}_4)_2 \cdot \text{H}_2\text{O}$	(Pre-treatment)	50	3541	156	1	5	75	-	-	1	4	86	55.13	-	-	-	-	86	55.13
		100	2025	155	4	19	57	-	-	4	8	92	59.35	-	-	-	-	92	59.35
		250	1235	155	1	12	47	-	-	-	8	68	43.87	-	-	-	-	68	43.87
		500	1053	153	4	19	52	-	-	4	10	89	58.17	-	-	-	-	89	58.17
	(Post-treatment)	50	1633	151	2	13	48	-	-	12	14	89	58.94	2	-	2	1.32	91	60.29
		100	1827	156	4	9	38	-	-	6	5	62	39.74	-	-	-	-	62	39.74
		250	2551	159	5	15	61	-	-	2	3	86	54.08	4	-	4	2.50	90	56.16
		500	1932	151	3	27	25	-	-	3	13	71	47.01	7	-	7	4.60	78	51.65

17

18 TC-Total Cells, TNAC-Total number of aberrant cells, -ve control-negative control, +ve control-positive control, Da- Delayed anaphase, Bk-Chromosomal break, St-  
 19 Sticky, Si-spindle inhibition, Aa-Abnormal anaphase, Am-Abnormal metaphase, Lg-laggard/s, Vg-vagrant/s, Bg- Chromatin bridge



1



2

3 **Figure 1.** UV-visible spectra of  $[\text{Co}(\text{NH}_3)_5\text{N}_3]\text{Cl}_2$ ,  $\text{KMnO}_4$  and  
4  $[\text{Co}(\text{NH}_3)_5\text{N}_3](\text{MnO}_4)_2 \cdot \text{H}_2\text{O}$

5

6

7

8

9

10

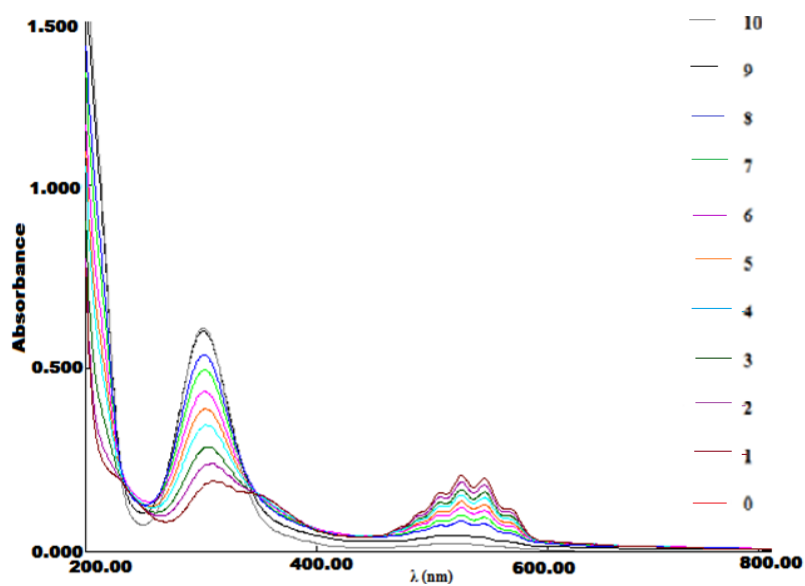
11

12

13

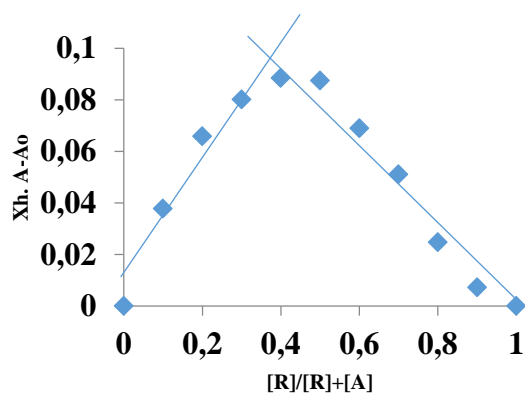
14

1



2

3



4

5 **Figure 2.** (a) UV/ vis titration spectra of receptor,  $[\text{Co}(\text{NH}_3)_5]\text{Cl}_2$  recorded in water ( $1$   
6  $\times 10^{-5}$  M) after the addition of 0-1equivalents of  $\text{KMnO}_4$ . (b) Job's plot (using  
7 continuous variation method of receptor with  $\text{KMnO}_4$  at  $\lambda_{\text{max}} = 313$  nm.  
8

9

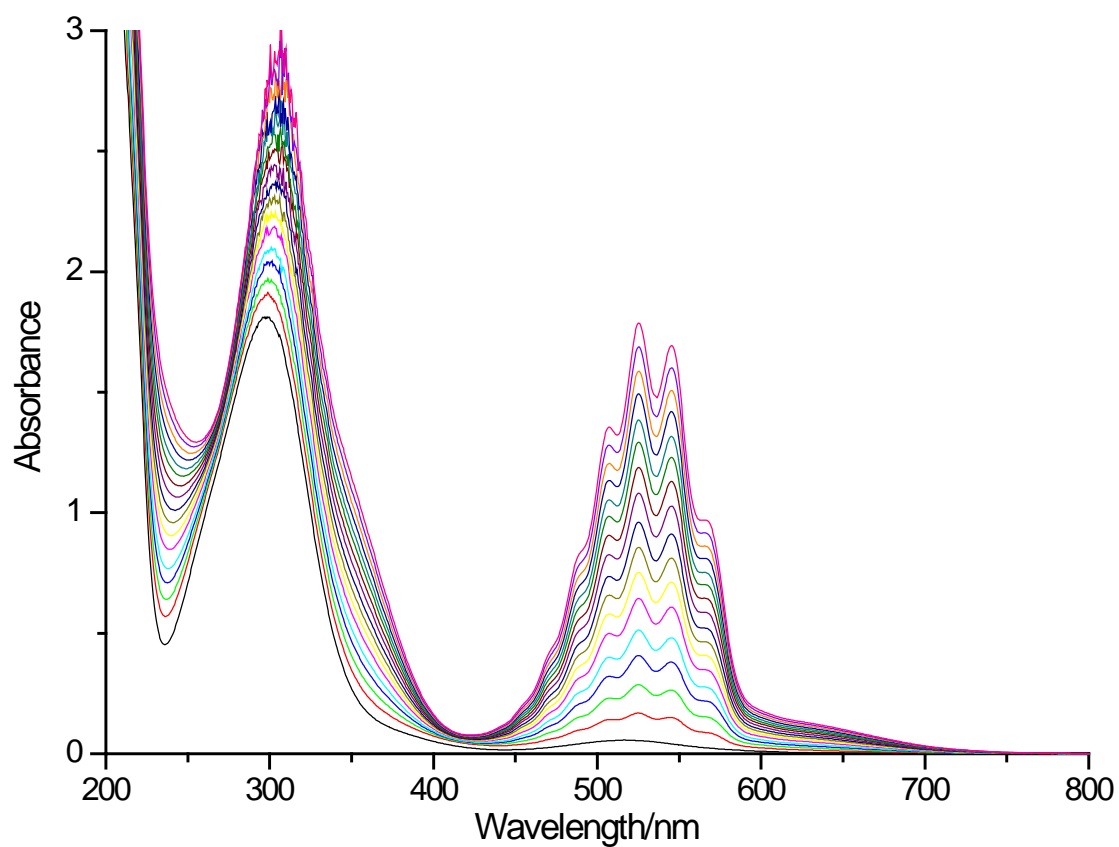
10

11

12

13

1



2

3

**Figure 3.** UV-Vis titration spectra of receptor,  $[\text{Co}(\text{NH}_3)_5\text{N}_3]\text{Cl}_2$  recorded in water ( $1 \times 10^{-4}$  M) after the addition of  $\text{KMnO}_4$  solution ( $1 \times 10^{-2}$  M)

4

5

6

7

8

9

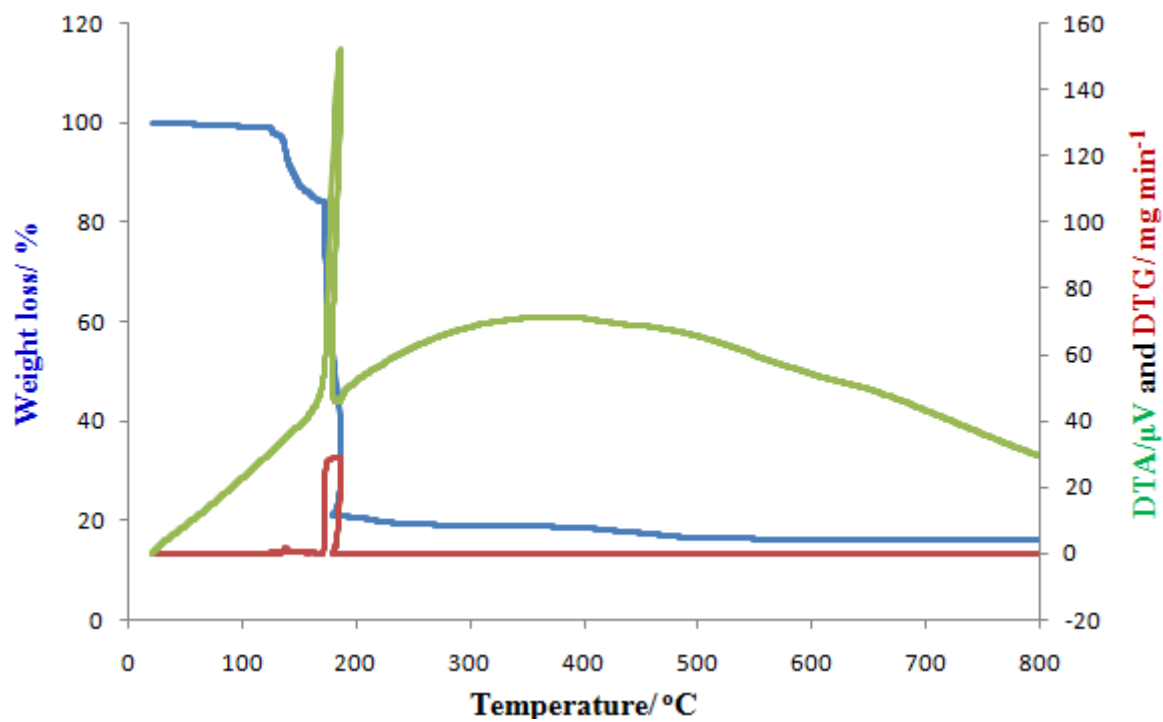
10

11

12

13

1



2

3

4 **Figure 4.** TG, DT and DTG analyses plot of  $[\text{Co}(\text{NH}_3)_5\text{N}_3](\text{MnO}_4)_2 \cdot \text{H}_2\text{O}$

5

6

7

8

9

10

11

12

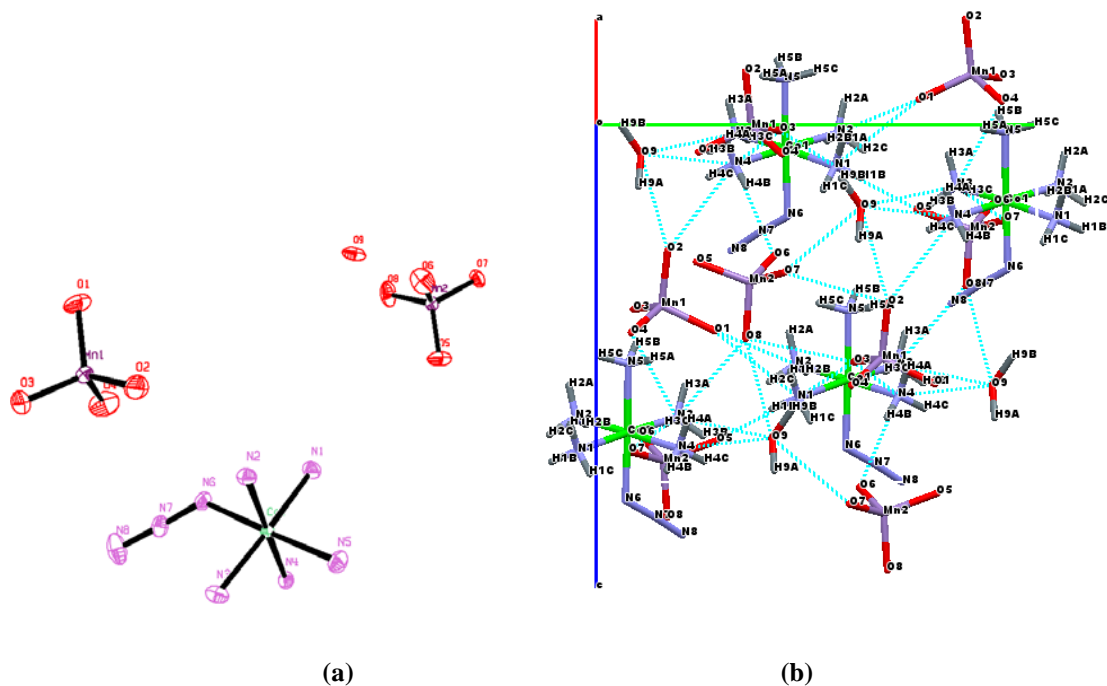
13

14

15

16

1



2

3

4 **Figure 5.** (a) ORTEP diagram of  $[\text{Co}(\text{NH}_3)_5\text{N}_3](\text{MnO}_4)_2 \cdot \text{H}_2\text{O}$  (30% ellipsoidal  
5 probability, H- atoms are omitted for clarity) (b) Crystal packing diagram (down to  $a^*$ -  
6 axis) for  $[\text{Co}(\text{NH}_3)_5\text{N}_3](\text{MnO}_4)_2 \cdot \text{H}_2\text{O}$  showing hydrogen bonding interactions. Dotted  
7 lines represent hydrogen bonds.

8

9

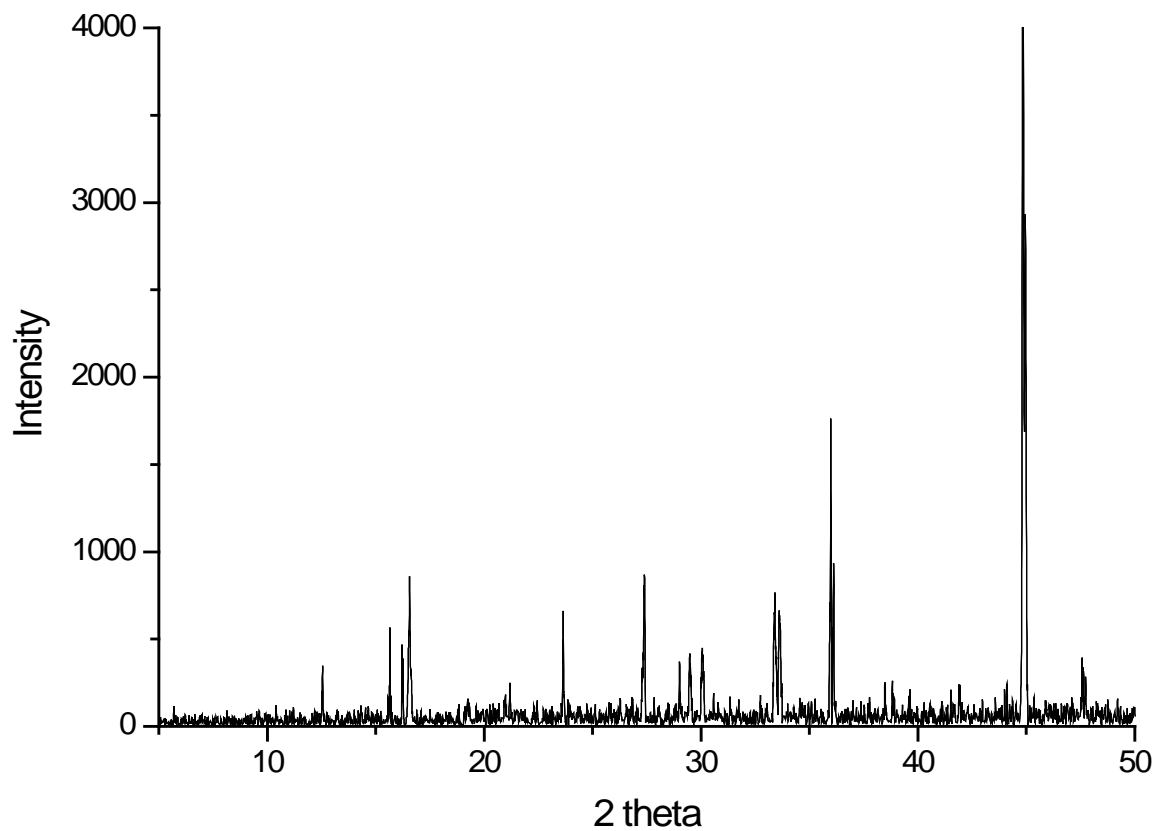
10

11

12

13

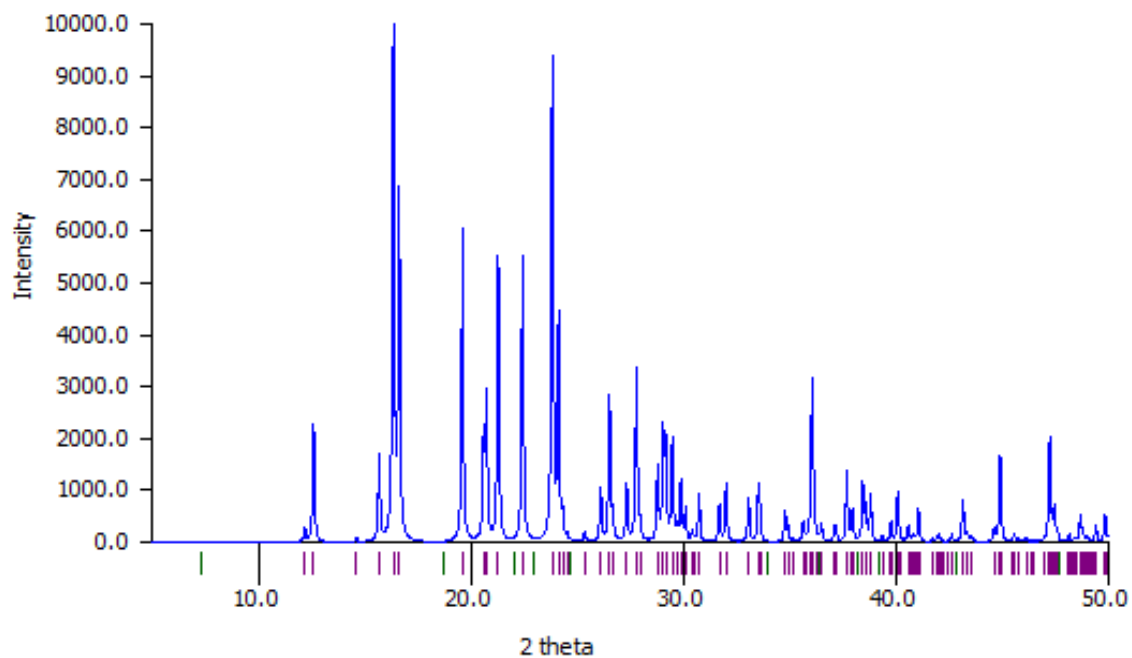
14



1

2

(a)



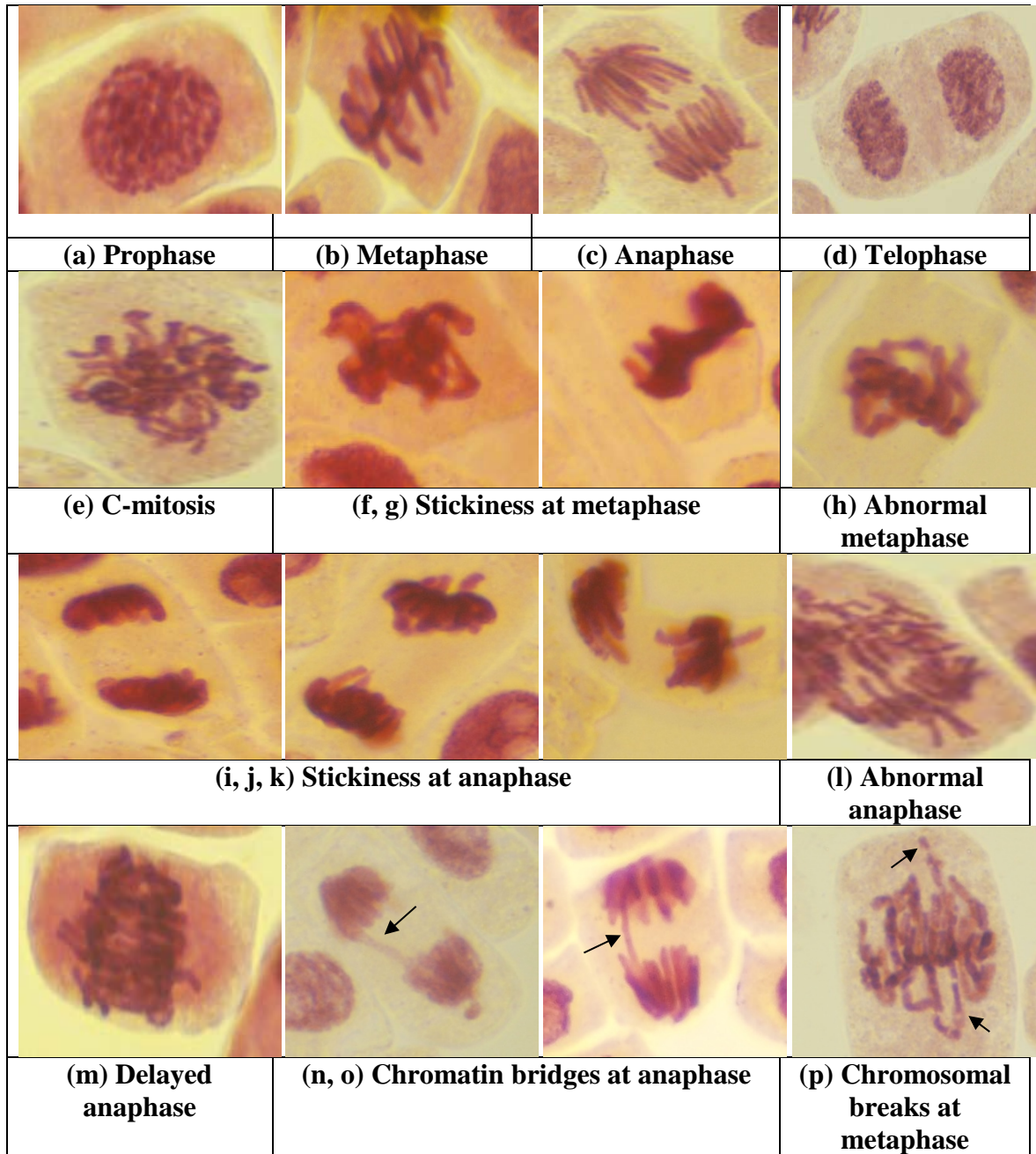
3

4

(b)

5 **Figure 6.** (a) XRD of  $[\text{Co}(\text{NH}_3)_5\text{N}_3](\text{MnO}_4)_2 \cdot \text{H}_2\text{O}$ , (b) XRD of  
 6  $[\text{Co}(\text{NH}_3)_5\text{N}_3](\text{MnO}_4)_2 \cdot \text{H}_2\text{O}$  obtained from cif

1



2

3 **Figure 7.** Various stages of mitotic division in root tip cells of *Allium cepa*; Normal  
 4 stages (a-d) and Stages with chromosomal aberrations (e-p).